Terahertz emission from lateral photo-Dember currents

G. Klatt[1],* F. Hilser[1], W. Qiao[1], M. Beck[1], R. Gebs[1], A. Bartels[1], K. Huska[2], U. Lemmer[2], G. Bastian[3], M.B. Johnston[4], M. Fischer[5], J. Faist[5], T. Dekorsy[1]

[1]*Department of Physics and Center for Applied Photonics, University of Konstanz, 78457, Germany*
[2]*Lichttechnisches Institut, Universität Karlsruhe (TH), 76128, Germany*
[3]*Faculty of Engineering, University of Applied Sciences Trier, Postfach 1826, 54208 Trier, Germany*
[4]*Clarendon Laboratory, Department of Physics, University of Oxford, Parks Road, OX1 3PU, Oxford, UK*
[5]*Institute for Quantum Electronics, ETH Zürich, 8093 Zürich, Switzerland*
**Gregor.Klatt@uni-konstanz.de*

Abstract: The photo-Dember effect is a source of impulsive THz emission following femtosecond pulsed optical excitation. This emission results from the ultrafast spatial separation of electron-hole pairs in strong carrier gradients due to their different diffusion coefficients. The associated time dependent polarization is oriented perpendicular to the excited surface which is inaptly for efficient out coupling of THz radiation. We propose a scheme for generating strong carrier gradients parallel to the excited surface. The resulting photo-Dember currents are oriented in the same direction and emit THz radiation into the favorable direction perpendicular to the surface. This effect is demonstrated for GaAs and $In_{0.53}Ga_{0.47}As$. Surprisingly the photo-Dember THz emitters provide higher bandwidth than photoconductive emitters. Multiplexing of phase coherent photo-Dember currents by periodically tailoring the photoexcited spatial carrier distribution gives rise to a strongly enhanced THz emission, which reaches electric field amplitudes comparable to a high-efficiency externally biased photoconductive emitter.

OCIS codes: (320.7130) Ultrafast processes in condensed matter, including semiconductors; (300.6495) Spectroscopy, terahertz.

References and links

1. M. Tonouchi, "Cutting-edge terahertz technology," Nat. Photonics **1**(2), 97–105 (2007).
2. B. Ferguson, and X.-C. Zhang, "Materials for terahertz science and technology," Nat. Mater. **1**(1), 26–33 (2002).
3. D. Mittleman, *Sensing with terahertz radiation*, Springer series in optical sciences (Springer, 2003).
4. G. Spickermann, F. Friederich, H. G. Roskos, and P. H. Bolívar, "High signal-to-noise-ratio electro-optical terahertz imaging system based on an optical demodulating detector array," Opt. Lett. **34**(21), 3424–3426 (2009).
5. X.-C. Zhang, and D. H. Auston, "Optoelectronic measurement of semiconductor surfaces and interfaces with femtosecond optics," J. Appl. Phys. **71**(1), 326–338 (1992).
6. R. Kersting, K. Unterrainer, G. Strasser, H. F. Kauffmann, and E. Gornik, "Few-Cycle THz Emission from Cold Plasma Oscillations," Phys. Rev. Lett. **79**(16), 3038–3041 (1997).
7. R. Huber, A. Brodschelm, F. Tauser, and A. Leitenstorfer, "Generation and field-resolved detection of femtosecond electromagnetic pulses tunable up to 41 THz," Appl. Phys. Lett. **76**(22), 3191–3193 (2000).
8. A. Dreyhaupt, S. Winnerl, T. Dekorsy, and M. Helm, "High-intensity terahertz radiation from a microstructured large-area photoconductor," Appl. Phys. Lett. **86**(12), 121114–3 (2005).
9. S. Verghese, K. A. McIntosh, S. Calawa, W. F. Dinatale, E. K. Duerr, and K. A. Molvar, "Generation and detection of coherent terahertz waves using two photomixers," Appl. Phys. Lett. **73**(26), 3824–3826 (1998).
10. E. Bründermann, D. R. Chamberlin, and E. E. Haller, "High duty cycle and continuous terahertz emission from germanium," Appl. Phys. Lett. **76**(21), 2991–2993 (2000).
11. R. Köhler, A. Tredicucci, F. Beltram, H. E. Beere, E. H. Linfield, A. G. Davies, D. A. Ritchie, R. C. Iotti, and F. Rossi, "Terahertz semiconductor-heterostructure laser," Nature **417**(6885), 156–159 (2002).
12. Q. Wu, and X.-C. Zhang, "Ultrafast electro-optic field sensors," Appl. Phys. Lett. **68**(12), 1604–1606 (1996).
13. A. Leitenstorfer, S. Hunsche, J. Shah, M. C. Nuss, and W. H. Knox, "Detectors and sources for ultrabroadband electro-optic sampling: Experiment and theory," Appl. Phys. Lett. **74**(11), 1516–1518 (1999).
14. H. Dember, "Über eine photoelektronische Kraft in Kupferoxydul-Kristallen," Z. Phys. **32**, 554 (1931).
15. T. Dekorsy, T. Pfeifer, W. Kütt, and H. Kurz, "Subpicosecond carrier transport in GaAs surface-space-charge fields," Phys. Rev. B **47**(7), 3842–3849 (1993).

#122424 - $15.00 USD Received 7 Jan 2010; revised 5 Feb 2010; accepted 15 Feb 2010; published 24 Feb 2010

16. T. Dekorsy, H. Auer, H. J. Bakker, H. G. Roskos, and H. Kurz, "THz electromagnetic emission by coherent infrared-active phonons," Phys. Rev. B **53**(7), 4005–4014 (1996).
17. P. Gu, M. Tani, S. Kono, K. Sakai, and X.-C. Zhang, "Study of terahertz radiation from InAs and InSb," J. Appl. Phys. **91**(9), 5533–5537 (2002).
18. J. N. Heyman, N. Coates, A. Reinhardt, and G. Strasser, "Diffusion and drift in terahertz emission at GaAs surfaces," Appl. Phys. Lett. **83**(26), 5476–5478 (2003).
19. M. P. Hasselbeck, L. A. Schlie, and D. Stalnaker, "Emission of electromagnetic radiation by coherent vibrational waves in stimulated Raman scattering," Appl. Phys. Lett. **85**(2), 173–175 (2004).
20. M. Nakajima, Y. Oda, and T. Suemoto, "Competing terahertz radiation mechanisms in semi-insulating InP at high-density excitation," Appl. Phys. Lett. **85**(14), 2694–2696 (2004).
21. R. Ascázubi, C. Shneider, I. Wilke, R. Pino, and P. S. Dutta, "Enhanced terahertz emission from impurity compensated GaSb," Phys. Rev. B **72**(4), 045328 (2005).
22. A. Urbanowicz, R. Adomavicius, and A. Krotkus, "Terahertz emission from photoexcited surfaces of Ge crystals," Physica B **367**(1-4), 152–157 (2005).
23. R. Ascázubi, I. Wilke, K. J. Kim, and P. Dutta, "Terahertz emission from $Ga_{1-x}In_xSb$," Phys. Rev. B **74**(7), 075323 (2006).
24. C. T. Que, T. Edamura, M. Nakajima, M. Tani, and M. Hangyo, "Terahertz Radiation from InAs Films on Silicon Substrates Excited by Femtosecond Laser Pulses," Jpn. J. Appl. Phys. **48**(1), 010211 (2009).
25. M. B. Johnston, D. M. Whittaker, A. Dowd, A. G. Davies, E. H. Linfield, X. Li, and D. A. Ritchie, "Generation of high-power terahertz pulses in a prism," Opt. Lett. **27**(21), 1935–1937 (2002).
26. A. Bartels, R. Cerna, C. Kistner, A. Thoma, F. Hudert, C. Janke, and T. Dekorsy, "Ultrafast time-domain spectroscopy based on high-speed asynchronous optical sampling," Rev. Sci. Instrum. **78**(3), 035107 (2007).
27. G. Klatt, R. Gebs, C. Janke, T. Dekorsy, and A. Bartels, "Rapid-scanning terahertz precision spectrometer with more than 6 THz spectral coverage," Opt. Express **17**(25), 22847–22854 (2009).
28. J. Shan, and T. Heinz, *Terahertz Radiation from Semiconductors*, Vol. 92 of Ultrafast Dynamical Processes in Semiconductors, Topics in App. Phys. (Springer-Verlag Berlin Heidelberg, 2004).
29. E. Castro-Camus, J. Lloyd-Hughes, and M. B. Johnston, "Three-dimensional carrier-dynamics simulation of terahertz emission from photoconductive switches," Phys. Rev. B **71**(19), 195301 (2005).
30. D. S. Kim, and D. S. Citrin, "Coulomb and radiation screening in photoconductive terahertz sources," Appl. Phys. Lett. **88**(16), 161117–3 (2006).
31. G. Zhao, R. N. Schouten, N. van der Valk, W. T. Wenckebach, and P. C. M. Planken, "Design and performance of a THz emission and detection setup based on a semi-insulating GaAs emitter," Rev. Sci. Instrum. **73**(4), 1715–1719 (2002).
32. P. C. Upadhya, W. Fan, A. Burnett, J. Cunningham, A. G. Davies, E. H. Linfield, J. Lloyd-Hughes, E. Castro-Camus, M. B. Johnston, and H. Beere, "Excitation-density-dependent generation of broadband terahertz radiation in an asymmetrically excited photoconductive antenna," Opt. Lett. **32**(16), 2297–2299 (2007).
33. M. B. Johnston, D. M. Whittaker, A. Corchia, A. G. Davies, and E. H. Linfield, "Simulation of terahertz generation at semiconductor surfaces," Phys. Rev. B **65**(16), 165301 (2002).
34. Y. A. Goldberg, and N. M. Shmidt, *Handbook series on semiconductor parameters, Volume 2: Ternary and Quaternary A_3B_5 Semiconductors* (World Scientific, 1999).
35. S. M. Sze, and K. K. Ng, *Physics of Semiconductor Devices* (Wiley-Interscience, 3rd edition, 2006).
36. M. Awad, M. Nagel, H. Kurz, J. Herfort, and K. Ploog, "Characterization of low temperature GaAs antenna array terahertz emitters," Appl. Phys. Lett. **91**(18), 181124 (2007).
37. G. Acuna, F. Buersgens, C. Lang, M. Handloser, A. Guggenmos, and R. Kersting, "Interdigitated terahertz emitters," Electron. Lett. **44**(3), 229–231 (2008).
38. F. Tauser, A. Leitenstorfer, and W. Zinth, "Amplified femtosecond pulses from an Er:fiber system: Nonlinear pulse shortening and selfreferencing detection of the carrier-envelope phase evolution," Opt. Express **11**(6), 594–600 (2003).

1. Introduction

The efficient generation of THz radiation in the frequency range from a few hundreds of gigahertz to several terahertz has been in the focus of scientific efforts in the past decade [1]. Efficient THz emitters are the premise for the development of high-sensitivity spectroscopy and high frame-rate imaging systems [2–4]. The generation of THz radiation can be divided into different categories, i.e. the generation of short THz pulses by employing ultrashort laser pulses [5–8], the generation of CW THz radiation from difference frequency mixing of two CW lasers [9] or THz lasers [10,11]. Sensitive time-domain THz spectroscopy systems employ broadband THz pulses generated from a femtosecond laser and a phase sensitive recording of the transient electric field via an electro-optic detection scheme [12,13]. The emitters used in time-domain THz spectroscopy can be divided into i) those based on nonlinear frequency conversion of the broad spectrum of a femtosecond laser into the THz frequency range or ii) those based on ultrafast charge carrier dynamics in semiconductors. The latter emitters are denoted as photoconductive emitters, since they typically employ a

#122424 - $15.00 USD Received 7 Jan 2010; revised 5 Feb 2010; accepted 15 Feb 2010; published 24 Feb 2010

static electric field which accelerates optically excited electron-hole pairs in a semiconductor. Photoconductive THz emitters are the main radiation source employed in the frequency range of a few terahertz.

A less common method for the generation of THz radiation is the photo-Dember effect [14]. This effect arises when electron-hole pairs are generated with a strong spatial gradient. This is the case when a highly absorbing semiconductor surface is optically excited resulting in a carrier gradient perpendicular to the surface. The difference of the diffusion constants of electrons and holes leads to the build-up of a space charge field between the diffusing carrier distributions. After a short time depending on the carrier gradient and the carrier densities [15,16], this space charge field couples the diffusion of electrons and holes giving rise to ambipolar diffusion. The build-up of the photo-Dember field itself is the origin of THz radiation [16–24]. THz radiation from the photo-Dember effect has been observed for many different strongly absorbing semiconductors with an intrinsic absorption length at a given excitation wavelength. Typically this absorption length is below 100 nm. The time-dependent dipole giving rise to the THz emission is oriented perpendicular to the excited surface, i.e. parallel to the optically generated carrier gradient (see Fig. 1(a)). This radiation - as well as the radiation generated through surface field screening - is coupled out very efficiently when the surface is excited under 45° and the THz radiation is detected in the direction of specular reflection [5]. However, a calculation of the total emitted intensity of an effective dipole oriented under 45° to the surface compared to the intensity of a dipole oriented parallel to the surface yields a ratio of 1/2 including the consideration of the total internal reflection. Hence the 45° geometry limits the efficiency of THz emitters based on photo-Dember polarizations oriented perpendicular to the surface [25]. Another limit is the magnitude of the initial carrier gradient which cannot be tailored but is given by the intrinsic absorption coefficient of the semiconductor at the excitation wavelength. Connected with the magnitude of the carrier gradient is the dynamics of the build-up of the Dember field which results in a small bandwidth of the emission typically limited to below 1 THz.

A better out coupling efficiency can be obtained if the carrier gradient is oriented parallel to the excited surface, because in this case the time-dependent dipole is oriented parallel to the surface (see Fig. 1(a),(b)). In this paper we demonstrate that such an approach indeed leads to efficient emission of THz radiation. A carrier gradient parallel to an excited surface is easily induced by partially shadowing the excitation area. The magnitude of this gradient can be significantly higher than that obtainable through the intrinsic absorption coefficient of the material in a conventional geometry, i.e. the carrier density drops within a few nanometers in the semiconductor. This effect increases the amplitude *and* the bandwidth of the THz emission significantly. We investigate the density dependence of the emitted THz emission for a single gradient produced at an excited metal-semiconductor edge. Furthermore we demonstrate strongly increased THz emission by multiplexing multiple carrier gradients with a periodic arrangement of either the metallization or structuring the semiconductor in a way that the THz emission from multiple photo-Dember currents add up phase coherently in the far field of the emitter.

#122424 - $15.00 USD Received 7 Jan 2010; revised 5 Feb 2010; accepted 15 Feb 2010; published 24 Feb 2010

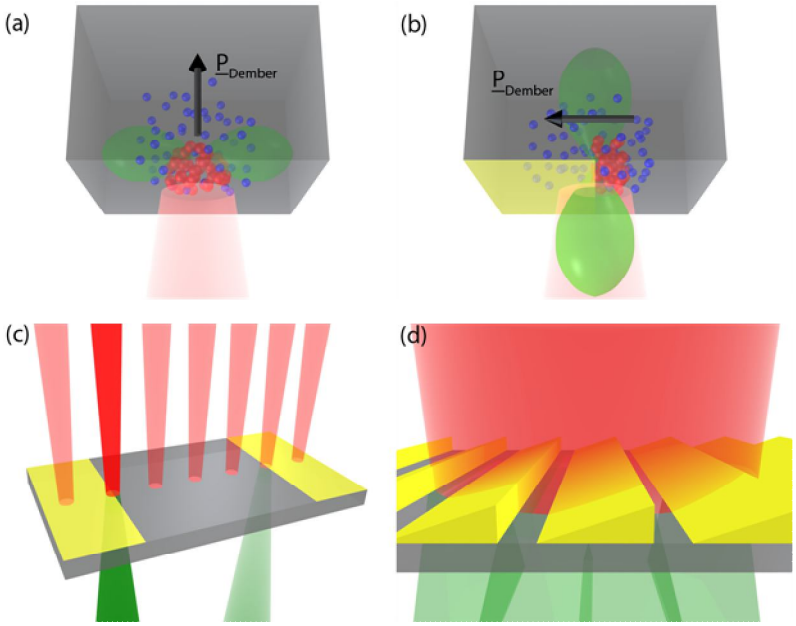

Fig. 1. (a), (b) Principle of the THz emission from lateral photo-Dember currents. In the case of a bare semiconductor surface the gradient of the photoexcited electrons (blue spheres) and holes (red spheres) and the resulting photo-Dember polarization P_{Dember} is directed perpendicular to the surface (a). In the case of a partially covered semiconductor surface a strong carrier gradient is achieved at the edge of a metalized stripe, resulting in a photo-Dember polarization parallel to the surface (b). In both pictures the green lobes indicate the dipole radiation patterns of the arising THz radiation. (c) Sketch of the sample with two gold stripes on GaAs used for the line scans shown in the inset of Fig. 2. The green cones show the forward direction of the resulting THz radiation. (d) Sketch of a multiplexed photo-Dember emitter as used for the data shown in Fig. 5.

2. Experimental setup

For the detection of THz transient we employ a set-up based on two asynchronously stabilized femtosecond lasers with 1 GHz repetition rate (Gigajet TWIN, Gigaoptics GmbH). This set-up is denoted as asynchronous optical sampling (ASOPS) and details have been reported elsewhere [26,27]. ASOPS operates without mechanical time delay with one laser exciting the THz photo-Dember emitter and the other is used for electro-optic probing of the THz transient in the time domain. A single scan of a 1 ns long THz transient is recorded in 500 µs. The THz radiation generated in forward direction through the emitter substrate is detected electro-optically in the far field. The laser used for the excitation of the emitters has a wavelength of 825 nm (1.50 eV photon energy) and 40 fs pulse duration. The maximum pulse energy of this high-repetition rate femtosecond laser is 0.6 nJ.

3. Results and discussion

The general principle for THz emission from lateral photo-Dember currents is sketched in Fig. 1(b). We first demonstrate this principle with two metallic stripes deposited onto a surface. The stripes are prepared by evaporation of 5 nm chromium and 80 nm gold and have a width of approximately 4 mm with a 10 mm gap in between (see Fig. 1(c)). At this thickness the gold film is opaque for the exciting light. The stripes are prepared on (100) oriented GaAs and on $In_{0.53}Ga_{0.47}As$ grown on InP. Figure 2 depicts two THz transients recorded when the maximum intensity of the Gaussian shaped optical excitation spot with 25 µm diameter is located at the metal edge (left or right edge, see schematic drawing in Fig. 1(c)). The inset of Fig. 2 shows the peak-to-peak amplitude of the emitted THz electric field derived from a series of transients acquired at different positions of the metal edge underneath the laser spot.

#122424 - $15.00 USD Received 7 Jan 2010; revised 5 Feb 2010; accepted 15 Feb 2010; published 24 Feb 2010

The time-domain data reveal a single cycle electromagnetic emission followed by some ringing. The ringing results from the high-bandwidth of our THz detection and the fact that frequencies above 4 THz experience a delayed propagation as phonon-polariton through the GaAs substrate of the emitter [27]. The sign of the electric THz field is reversed when the laser spot is centered on the right or left edge of the metal stripe, respectively. This sign reversal is a clear indication that the emitting polarization changes its sign. Since the origin of the photo-Dember polarization is the faster diffusion of the electrons into the unexcited area below the metallization, the polarization flips polarity between the left and the right metal edge. The frequency content of the THz transients will be discussed later. The line scan across the metal stripe shows that the THz emission peaks when the laser spot is centered on the edge of the metal stripe. The full width at half maximum of the peak-to-peak THz amplitude is 75 µm which results from the convolution of the metal edge with the Gaussian laser profile. A much weaker emission is observed when the laser spot is located fully on the bare semiconductor surface. This emission is the residual radiation of the dipole oriented perpendicular to the surface caused by surface field screening which is collected by the large collection angle of 53° of the off-axis parabolic mirrors. No emission is observed when the laser pulse is fully located on the opaque metallization. In order to rule out that the THz emission observed at the edge of the metal stripe stems from lateral components of Schottky barrier fields of the metal, we performed additional experiments with a thick insulating layer of LiF (300 nm) under the metal. The spatial dependence of the THz emission remains the same.

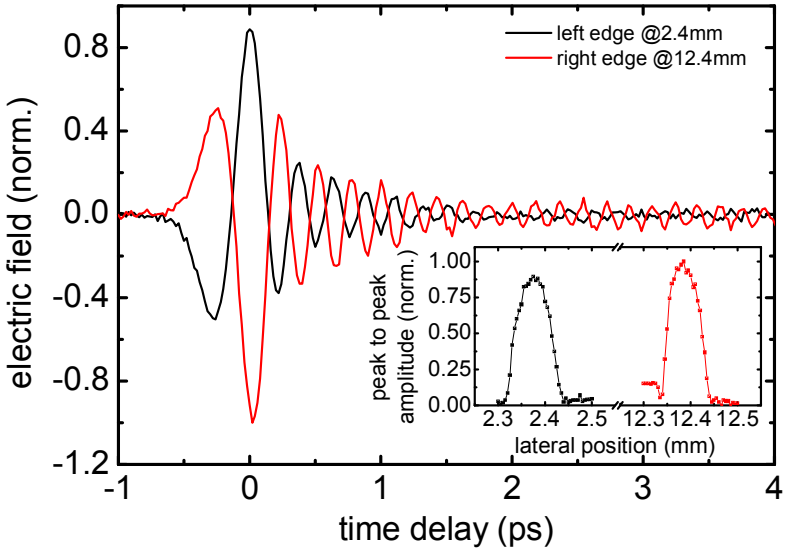

Fig. 2. THz transients emitted from the left (black) and right (red) metal-semiconductor edge. Left and right are defined as in the schematic drawing shown in Fig. 1(c). The transients are normalized to the maximum electric field value at the right edge. The inset shows the peak-to-peak amplitude of the emitted THz electric field when the metal-semiconductor edge is translated underneath the laser spot. The line scans are normalized to the peak-to-peak amplitude at 12.39 mm.

For the scalability of THz emitters the behavior under strong excitation densities is of prime importance. Photoconductive THz emitters are well known to saturate at high excitation densities due to screening of the static applied bias [28–30]. In addition photoconductive THz emitters suffer from high dark-currents when biased with high voltages [31,32]. Figure 3 depicts the excitation density dependence of the THz emission for the same sample as used in Fig. 1. The excitation density is varied over three orders of magnitude. Each data point marks the peak-to-peak amplitude of the emitted electric field when the maximum intensity of the optical excitation beam is located exactly at the metal edge. The data are recorded with 3

#122424 - $15.00 USD Received 7 Jan 2010; revised 5 Feb 2010; accepted 15 Feb 2010; published 24 Feb 2010

different focusing lenses (focal lengths of 150 mm, 250 mm, and 750 mm) yielding spot diameters of 25 µm, 55 µm, and 170 µm, respectively. At every spot size the average laser power is varied between 25 mW and 500 mW. The carrier density is calculated from the known absorption coefficient and laser fluence. The peak-to-peak THz amplitude is weighted linearly with the excitation area. This allows to compare the density dependence of the photo-Dember THz emission with the emission from a large area photoconductive emitter with interdigitated electrodes and an external bias (PC-emitter) [8], which is depicted in the inset of Fig. 3. The photoconductive emitter is biased with 10 V, which corresponds to an electric field of 20 kV/cm. In this case the whole excited spot area contributes to the THz emission, while for the single metal-semiconductor edge photo-Dember emitter only the carrier density along one section of the spot profile contributes. For the PC-emitter we expect at the given range of excitation densities a linear increase of THz amplitude which is experimentally verified. For the photo-Dember emitter the theoretical emission curve has yet to be determined. At the lowest carrier densities (10^{16} cm^{-3}) we verified the build-up of the photo-Dember polarization through Monte Carlo simulations [29,33]. Higher densities were not simulated due to the limits of computing power of the PC used. We expect at carrier densities larger than 10^{18} cm^{-3} a saturation due to the limited density of states in the conduction band (4×10^{17} cm^{-3}) of GaAs at this excitation wavelength. A full analysis would require the calculation of all real-space and k-space scattering events at these densities including the determination of transient polarizations, screening, plasmon-phonon dynamics and transient diffusion dynamics. Experimentally we observe a linear increase of the THz emission up to 10^{17} cm^{-3} carrier density and a sublinear increase for higher densities in accordance with our estimate.

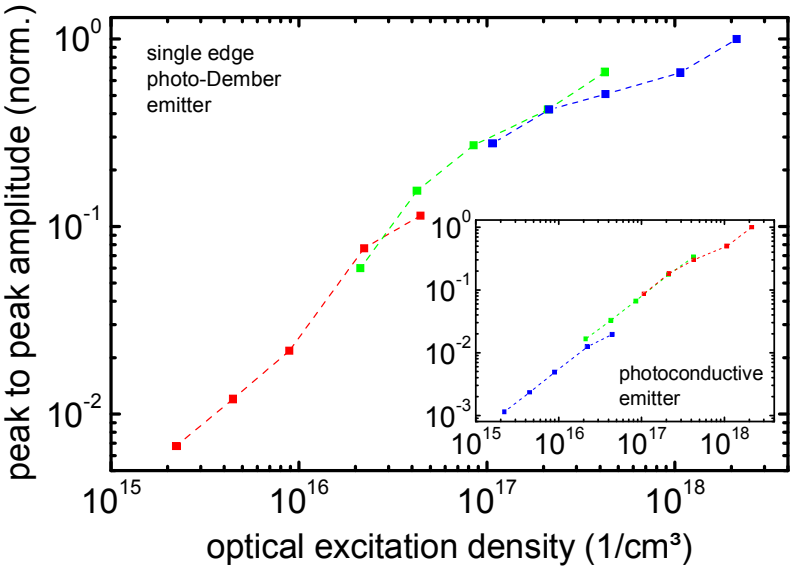

Fig. 3. Excitation density dependence of the THz emission of the same sample as used in Fig. 2. The data are normalized to the peak-to-peak amplitude at the highest excitation density. The different colors refer to different spot sizes as given in the text. The inset shows the excitation density dependence of a large area photoconductive emitter with interdigitated electrodes. Again the data are normalized to the value at the highest excitation density. The descriptions of the axis are the same as in the main plot.

One important parameter for the efficiency of photo-Dember emitters is the ratio of diffusion constants of electrons and holes. In thermal equilibrium the diffusion constant is related to the mobility via the Einstein relation $D_i/\mu_i=k_bT_i/e$ with D_i the diffusion coefficient, μ_i the mobility, k_b the Boltzmann constant and T_i the temperature of the carrier distribution function (the index i stands for electrons and holes, respectively). Hence a favorable material

#122424 - $15.00 USD Received 7 Jan 2010; revised 5 Feb 2010; accepted 15 Feb 2010; published 24 Feb 2010

would have high electron mobilities and low hole mobilities (or vice versa). In order to study the effect of different mobilities we compare the THz emission from GaAs substrates with $In_{0.53}Ga_{0.47}As$. In thermal equilibrium the ratio of the mobilities of electrons in the Γ-valley and heavy holes is about 21 (8500 cm^2/Vs and 400 cm^2/Vs) for undoped GaAs and 40 (12000 cm^2/Vs and 300 cm^2/Vs) for undoped $In_{0.53}Ga_{0.47}As$ [34,35]. Since the carrier distributions are not in thermal equilibrium these values are different after pulsed laser excitation and provide only a rough estimate for this effect.

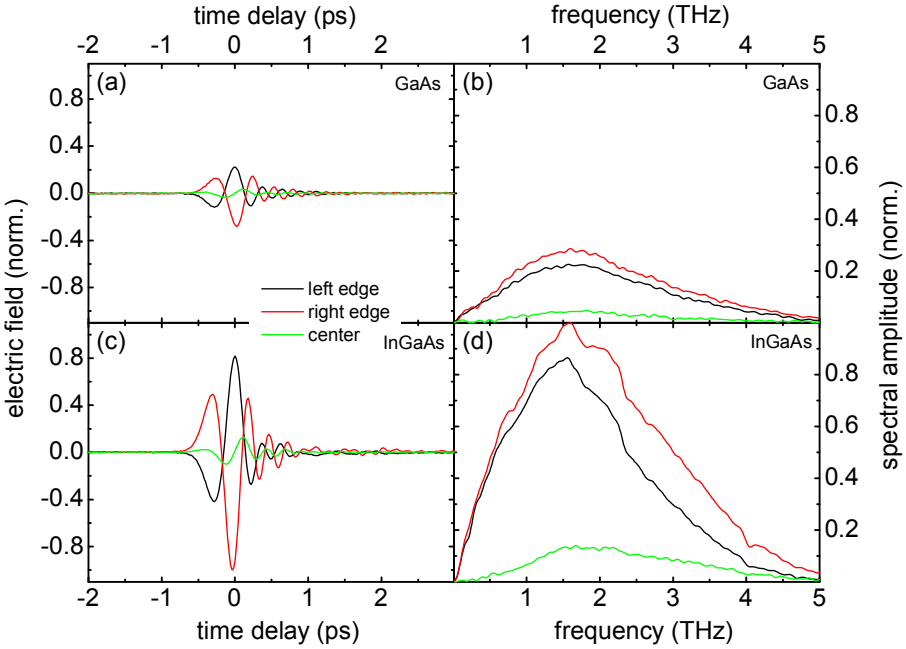

Fig. 4. Time-domain THz emission (left - a, c) and corresponding Fourier amplitude spectra (right - b, d) of the left (black) and right (red) metal-semiconductor edge on GaAs (top - a, b) and InGaAs (bottom - c, d). Additionally the transients and Fourier amplitude spectra of the bare substrate are shown in every graph (green). The transients and Fourier amplitude spectra are normalized to the right metal-semiconductor edge on GaAs.

Figures 4(a) and (b) show the THz transients and their Fourier spectra measured exactly at the left and right metal-semiconductor edge (black and red line) and at the bare GaAs substrate material (green line). The optical power is 500 mW and the spot diameter is 55 µm for all measurements. This corresponds to an excitation density of 4.25×10^{17} cm^{-3} in GaAs. In Figs. 4(c) and (d) InGaAs is used under the same conditions. The emitted electric fields of the left and right metal-semiconductor edges point again in opposite directions. The strongest emission stems from the right metal-semiconductor edge on the InGaAs substrate which is a factor of 3.5 larger than the maximum emission from the GaAs sample described above. Compared to a PC-emitter the amplitude of the photo-Dember emitter is only 12 times smaller under the same excitation fluence. When making this comparison one has to keep in mind that only one section of the spot profile contributes to the THz emission, whereas for a PC-emitter the THz radiation is generated over the whole excited area. Concerning the bandwidth (full width half maximum, FWHM) as well as the peak frequency the photo-Dember emitter shows a better performance than the PC-emitter (PC-emitter: FWHM 1.9 THz, peak frequency 1.18 THz, photo-Dember emitter: FWHM 2.47, peak frequency 1.58 THz). These excellent spectral values were unexpected when considering the low peak frequency of photo-Dember emitters reported so far [16,17,20–24]. We expect that the emission from the InGaAs sample can be increased by excitation close to the band edge. At the used excitation energy of 1.5 eV the electrons have significant excess energy (E_g = 0.74 eV). Hence strong intervalley

#122424 - $15.00 USD Received 7 Jan 2010; revised 5 Feb 2010; accepted 15 Feb 2010; published 24 Feb 2010

scattering of electrons sets in, which reduces the mobility of the electrons in comparison to those of the holes. We believe that this effect can be overcome by excitation close to the band edge.

Finally we demonstrate that multiple optically excited carrier gradients can be added in order to increase the THz amplitude. A simple array of metal stripes covered by the optical excitation would not lead to THz radiation in the far field, since the THz radiation from the two directions of the gradients would interfere destructively. Hence, we use the same concept which has been employed for PC-emitters [8,36,37] where in every second gap between electrodes optical excitation is avoided. In the case of PC-emitters this gives rise to coherent superposition of THz radiation generated from unidirectional acceleration of charge carriers. In the case of multiplexed photo-Dember emitters one has to avoid every second carrier gradient so that the resulting carrier gradients are unidirectional. There exist many different approaches how this can be achieved: One way is to vary the thickness of every metal mask stripe to control the absorbed light in the semiconductor as sketched in Fig. 1(d). A wedged metal stripe generates a strong gradient at its thick edge, while a weak gradient is obtained at the thin edge, because more light transmits through the mask when the metal thickness gets into the few nm range.

Figure 5 compares a multiplexed photo-Dember emitter (red line) manufactured as described above with a PC-emitter (black line). The multiplexed photo-Dember emitter is manufactured on the same InGaAs substrate that was used for the single metal-semiconductor edge. The emitter has a size of 200 x 200 µm and consists of 40 wedged stripes. Figure 5(a) shows the THz transients, Fig. 5(b) the corresponding Fourier spectra. The inset of Fig. 5(b) shows the same Fourier data as the main plot, but not normalized and on a logarithmic scale. The peak-to-peak electric field of the multiplexed photo-Dember emitter is one third of the PC-emitter. Consequently, the areas under the Fourier amplitude spectra also differ about the same factor (x 3.8).

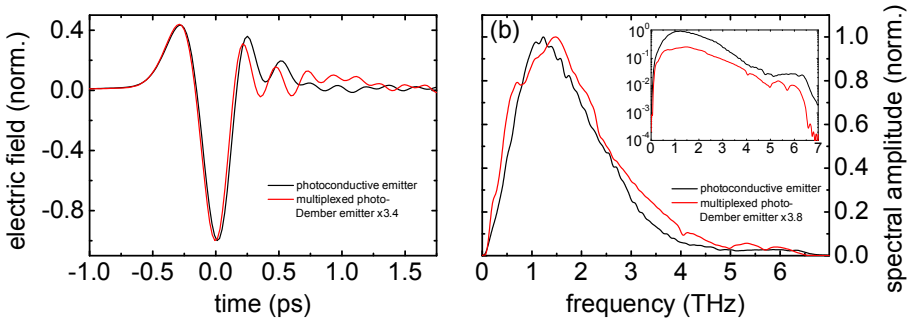

Fig. 5. Comparison of a large area photoconductive emitter with interdigitated electrodes with a multiplexed photo-Dember emitter. The micro-structure of the multiplexed photo-Dember emitter is shown in Fig. 1(d). Figure (a) shows the normalized THz transients, (b) the normalized Fourier amplitude spectra. The inset shows the same data not normalized for absolute comparison on a log scale.

In order to further improve the performance of the multiplexed photo-Dember emitters, different routes are feasible: From a microscopic point of view, maximum performance is achieved through a maximum difference between the electron and hole mobilities. This goal can be reached by choosing the optimum substrate material in combination with the appropriate laser wavelength for excitation of electrons and holes. From a macroscopic point of view, the fabrication of multiple sharp unidirectional carrier gradients offers a large room for further improvements. One way is the wedged metal stripe approach described above. This can be further improved by narrower stripe spacing. Different approaches for generating unidirectional carrier gradients could be based on a combination of selective etching and metal masking. These ideas could further improve these emitters by more than a factor of 5 so that they can surpass the performance of PC-emitters.

#122424 - $15.00 USD Received 7 Jan 2010; revised 5 Feb 2010; accepted 15 Feb 2010; published 24 Feb 2010

4. Conclusion

In summary, we have demonstrated the first THz emission from lateral photo-Dember currents in forward direction from a semiconductor. The THz electric fields obtained from multiplexed photo-Dember currents are already comparable to the best currently available large area photoconductive emitters with interdigitated electrodes and external bias. The concept to generate THz radiation by lateral photo-Dember currents offers several advantages compared to other type of emitters. Scalability towards large excited areas with high-energy excitation pulses, e.g. from amplified laser systems, opens the way towards powerful high-bandwidth THz emission. Compared to frequently employed photoconductive emitters no external bias is necessary. These emitters could be directly attached to the end of an optical fiber opening possibilities for compact THz systems. Under excitation with 1.55 μm with a femtosecond fiber [38] in combination with InGaAs a higher efficiency than reported here is expected, since the detrimental effect of strong intervalley scattering would be suppressed.

Acknowledgments

This research is supported by the Landesstiftung Baden-Württemberg. Financial support of the Center for Applied Photonics (CAP) is gratefully acknowledged.

#122424 - $15.00 USD Received 7 Jan 2010; revised 5 Feb 2010; accepted 15 Feb 2010; published 24 Feb 2010